



## Mantle plumes: Thin, fat, successful, or failing? Constraints to explain hot spot volcanism through time and space

Ichiro Kumagai,<sup>1,2</sup> Anne Davaille,<sup>1,3</sup> Kei Kurita,<sup>2</sup> and Eléonore Stutzmann<sup>1</sup>

Received 20 June 2008; revised 9 July 2008; accepted 11 July 2008; published 16 August 2008.

[1] Density heterogeneities in the mantle influence the dynamics of mantle upwellings and therefore modify plume characteristics. Using analog laboratory experiments, we explore the dynamics of “thermo-chemical” plumes containing both thermal and chemical density anomalies inherited from a stratified boundary layer at the base of the mantle. Because all plumes cool by thermal diffusion as they rise, a chemically composite thermal plume will eventually attain a level of neutral buoyancy, at which it will begin to “fail”. Separation within the plume will occur, whereby the chemically denser material will start to sink back while the heated surrounding mantle keeps rising. It more generally implies that 1) mantle plumes are not necessarily narrow and continuous throughout the mantle but can be fat and patchy such as Iceland, 2) a hot mantle region may not be buoyant and rising, but on contrary may be sinking, and 3) mantle plumes dynamics are strongly time-dependent. **Citation:** Kumagai, I., A. Davaille, K. Kurita, and E. Stutzmann (2008), Mantle plumes: Thin, fat, successful, or failing? Constraints to explain hot spot volcanism through time and space, *Geophys. Res. Lett.*, 35, L16301, doi:10.1029/2008GL035079.

### 1. Introduction

[2] Given the mantle size and physical properties, and the temperature difference between the cold surface of our planet and the core-mantle boundary (CMB), thermal convection and hot instabilities should develop in the mantle [e.g., Schubert *et al.*, 2001]. In that case, hot spot volcanism [Wilson, 1963] will result from the impact under the lithosphere of these hot instabilities [Morgan, 1971]. In a homogeneous fluid, their morphology should be that of mushroom-shape plumes, with a big head over a narrower stem [Morgan, 1971; Griffiths and Campbell, 1990; Sleep, 1990]. The former would produce traps on the Earth’s surface while the latter would generate long volcanic tracks, therefore explaining first order observations on a number of hot spots [Richards *et al.*, 1989]. However, as data on hot spots increased, it became clear that all of it cannot be explained by this simple model: there are probably several types of hot spot on Earth [Morgan, 1978; Davaille, 1999; Courtillot *et al.*, 2003].

[3] The presence of density heterogeneities in the mantle is probably a key feature to relate the diversity of hot spot observations to mantle convection [Davaille, 1999; Farnetani and Samuel, 2005]. Laboratory and numerical studies have shown that the interplay of density heterogeneities and thermal convection produces hot instabilities of widely differing morphologies such as anchored plumes, piles and domes, secondary plumes, and composite “thermo-chemical” plumes (for a review, see Davaille *et al.* [2005]). They are characterized by a strong time-dependence with typical time-scales of 100–300 Ma [Le Bars and Davaille, 2004b; Lin and van Keken, 2005; Samuel and Bercovici, 2006] and could develop for mantle density anomalies lower than 2%.

[4] We focus here on the 3D morphology and evolution of thermo-chemical plumes generated from a mantle thermal boundary layer (“TBL”) which initially is stably stratified in composition. Laboratory experiments allow us to relax the axisymmetric hypothesis used in high resolution numerical models [Lin and van Keken, 2005; Samuel and Bercovici, 2006]. We report more diverse plume morphology and detailed information on the time evolution of the thermo-chemical plumes characteristics. In particular, our results could explain key observations such as the patchy nature of the tomographically imaged anomalies of elastic wave speed beneath Iceland and the large (~140–200 K) decrease in this plume’s excess temperature during the past 60 Ma.

### 2. Successful and Failing Thermo-chemical Plumes

[5] In our experiments a thermal plume was generated by a heated disk on the base of a plexiglas tank filled with sugar syrup whose viscosity, like that of mantle materials, decreases with increasing temperature. There is no point-source bottom heater at the base of the mantle, which is continuously heated on all its lower boundary by the core. But to use such localized heat sources allows us to study more quantitatively a plume time history. So, at time  $t = 0$ , the heater was turned on, and either kept at constant power throughout the experiment (Figures 1 and 2a), or switched off after a while (Figure 2b). The former situation would corresponds to an anchored plume [Namiki and Kurita, 1999; Davaille, 1999; Jellineck and Manga, 2002], while the latter mimics the episodic release of plumes from a TBL uniformly heated from below: in this case, thermal plumes become disconnected from the heat source once they have exhausted all the hot TBL material [Le Bars and Davaille, 2004a; Davaille and Vatteville, 2005].

[6] Using a new technique [Kumagai *et al.*, 2007], we measured simultaneously the temperature, composition, and

<sup>1</sup>Institut de Physique du Globe de Paris, UMR7154, Université Paris Diderot, CNRS, Paris, France.

<sup>2</sup>Earthquake Research Institute, University of Tokyo, Tokyo, Japan.

<sup>3</sup>Laboratoire FAST, UMR7608, Université Pierre et Marie Curie, Université Paris-Sud 11, CNRS, Orsay, France.

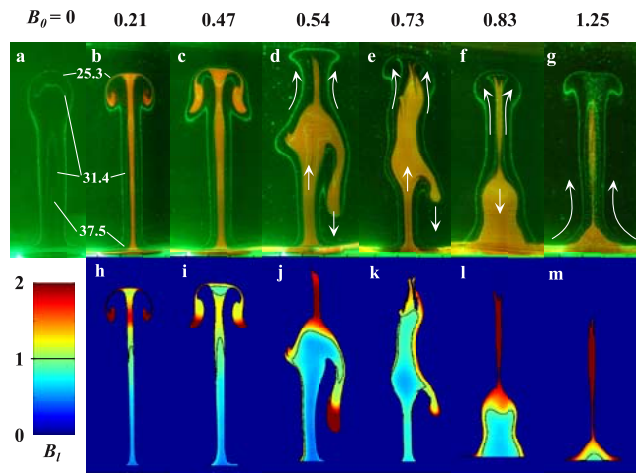


**Figure 1.** Morphology of thermo-chemical plumes as a function of the increasing initial Buoyancy ratio  $B_0$ . The cross section of the tank is illuminated by a 532 nm laser sheet. The compositional heterogeneity is dyed in Rhodamine B (orange). The bright green lines are isotherms (25.3, 31.4, 37.5°C). (a) Thermal starting plume, (b, c) thermo-chemical plumes with small  $B_0$ , (d–f) failing plumes, and (g) thermal starting plume generated from the chemical interface with small entrainment. (h–m) Distribution of the local buoyancy ratio  $B_l$  calculated through the image analysis of Figures 1b–1g.

velocity fields on a 2D vertical cross-section containing the plume axis, which was illuminated by a narrow sheet of laser light of 532 nm wavelength. The thermal field was measured by seeding the fluid with thermochromic liquid crystals which brighten at three different calibrated temperatures (bright lines in Figures 1 and 2). The velocity field was measured by particle-image velocimetry using small nylon tracer particles. Finally, the compositionally denser material (CDM) was dyed with Rhodamine B, which appears orange under the laser illumination (Figures 1 and 2). 26 experiments were performed in which the heating rate, and the density anomaly and thickness of the CDM were systematically varied, so that the parameters characterizing the system dynamics were over the range of values relevant for the mantle (Table 1).

[7] The instabilities which develop are composite plumes, made of both CDM and upper layer material. Their morphology and time-evolution depend on the initial buoyancy ratio  $B_0$ , the key parameter of the problem:

$$B_0 = \Delta\rho_{\text{Xeff}}/\rho\alpha\Delta T_{\text{eff}}$$

where  $\rho$  is the density,  $\alpha$  is the thermal expansion, and  $\Delta\rho_{\text{Xeff}}$  and  $\Delta T_{\text{eff}}$  are the average chemical density and temperature anomalies of the composite hot plume compared to the ambient fluid.

[8] Figure 1 shows the thermo-chemical plume morphology at a given height, as  $B_0$  increases. There are two end-members: for  $B_0$  tending towards 0, the mushroom-shaped purely thermal plume is reproduced [Griffiths and Campbell, 1990](Figures 1a and 1b). For  $B_0$  greater than 1, the thermal effects will never counterbalanced the chemically denser anomaly. Hence only the upper part of the TBL becomes

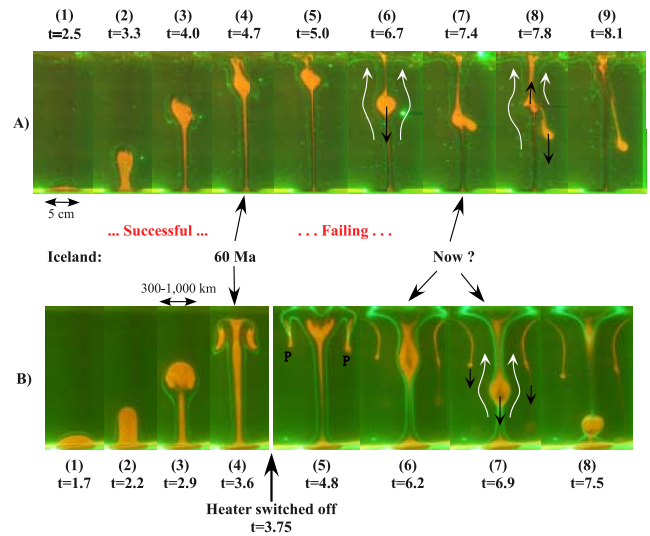


**Figure 2.** Successful and failing plumes and time dependence. (a) Evolution of thermo-chemical plume ( $B_0 = 0.67$ ). The power is constant during this experiment. Here  $t$  is time normalized by the onset time of doming ( $t_{cr} = 66$  sec). Note that a disintegration of the chemical blob (8) causes a second thermal impact at the surface (9). (b) Evolution of thermo-chemical plume ( $B_0 = 0.47$ ;  $t_{cr} = 160$  sec). The power is turned off at  $t = 3.75$ . By cooling, the core of the plume head, which is still hotter than the ambient fluid, descends through the pipe. Note that circumferential instability occurs around the plume head (see the images after  $t = 4.8$ ) and several tiny plumes (P) are generated and sinking to the bottom. The isolated hot thermo-chemical blob is failing (descending) in the later stage.

unstable, deforming the CDM layer into a cusp and entraining a thin CDM filament by viscous coupling [Davaille, 1999; Jellinek and Manga, 2002; Kumagai et al., 2007] (Figure 1g). For intermediate  $B_0$ , complex shapes are observed (Figures 1c–1f), where hot fluid is rising, but also sometimes sinking (Figures 1d–1f). The thermal anomaly associated with these structures is often broader than in the case of a purely thermal plume. From the measured compositional and thermal fields, we can calculate the

**Table 1.** Dynamics Parameters for the Laboratory Experiments and for the Earth's Mantle<sup>a</sup>

Parameters	Laboratory Experiments	Mantle
$Ra = \alpha g \Delta T_{\text{eff}} H^3 / \kappa \nu_m$	$2.2 \times 10^6 - 9.6 \times 10^6$	$> 10^6$
$\gamma_p = \nu_m / \nu_{\text{hot}}$	5 – 150	$1 - 10^3 ?$
$\gamma_{\text{ref}} = \nu_m / \nu_{\text{ref}}$	0.4 – 1.8	$\sim 1 ?$
$a = H / h_{\text{CDM}}$	17 – 169	$> 10 ?$
$B_0$	0 – 1.30	0 – 10 ?
$h_{\text{TBL}} / h_{\text{CDM}}$	1 – 4.20	1 – 10 ?
$\Delta\rho_{\text{X}} / \rho$	0.0 – 2.35%	0 – 10% ?

<sup>a</sup>The Rayleigh number,  $Ra$ , gives the vigour of convection, where  $H$  is the total thickness of fluid,  $\kappa$  is the heat diffusivity, and  $\nu_m$  is the kinematic viscosity of the top layer.  $\gamma_p$  is the kinematic viscosity ratio of the top layer to the hotter plume.  $\gamma_{\text{ref}}$  is the reference kinematic viscosity ratio of the top layer to the CDM at room temperature  $\nu_{\text{ref}}$ .  $h_{\text{CDM}}$  designates the thickness of the CDM layer, and  $h_{\text{TBL}}$  is the hot thermal boundary layer thickness which depends on  $Ra$ . Four parameters are necessary to characterize the dynamics of thermo-chemical plumes in the two layer system:  $Ra$ ,  $\gamma_B$ ,  $a$ ,  $B_0$  [Davaille, 1999; Davaille et al., 2005].

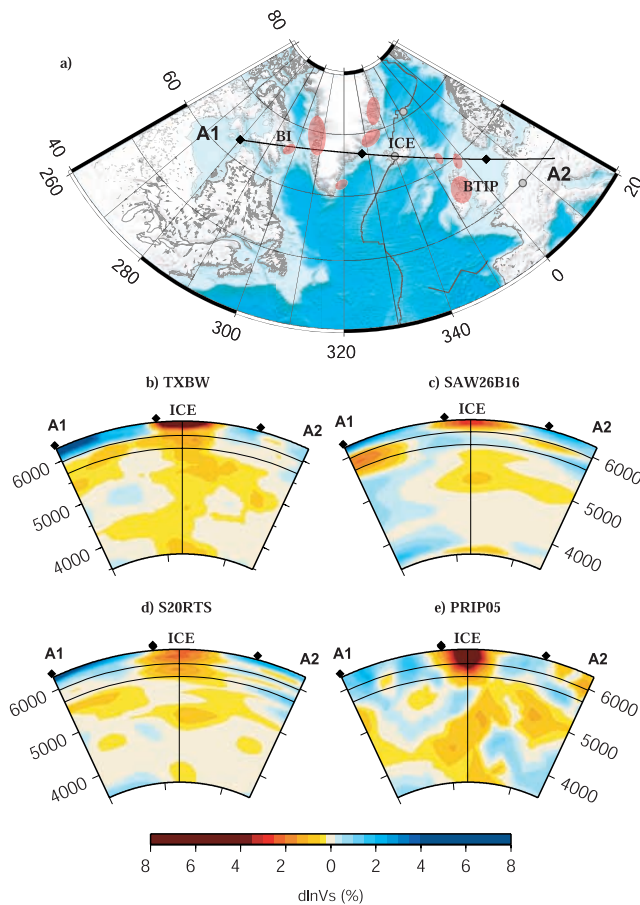


**Figure 3.** Recent seismic tomography models for S-wave beneath the Icelandic region. (a) Map of the North Atlantic. Indicated are Iceland (ICE), Baffin Island (BI) and the British Tertiary Igneous Province (BTIP). The pink areas show the extent of the trap events at 60 Ma. S-wave tomographic models: vertical cross-sections in the mantle along the profile A1–A2 indicated in Figure 3a: (b) model by *Grand et al.* [1997], (c) model by *Mégnin and Romanowicz* [2000], (d) model by *Ritsema et al.* [1999], and (e) model by *Montelli et al.* [2006].

local buoyancy ratio  $B_1(x,y,z) = \Delta\rho_x(x,y,z)/\rho\alpha[T(x,y,z) - T_0]$  anywhere in the tank (Figures 1h–1m). Comparison between this buoyancy field and the velocity field shows that the separation between active rising and sinking regions occurs for  $B_1 = 1.0$ . The maximum height of this “neutral buoyancy” level is a decreasing function of  $B_0$  [*Le Bars and Davaille, 2004a; Samuel and Bercovici, 2006; Kumagai et al., 2007*] (Figure 1).

[9] If the morphology of a composite plume depends on  $B_0$ , it also strongly depends on time (Figure 2 and Animations S1–S3<sup>1</sup>). After the heater is switched on, the TBL grows by thermal diffusion, until it becomes unstable. For intermediate  $B_0$ , the CDM is sufficiently heated to become buoyant and rise as an active part of the instability. Owing to the lower viscosity of the hot material, small-scale instabilities can develop in the CDM and gather to

form part of the plume head [*Davaille et al., 2005; Lin and van Keken, 2005*] (Figures 2a (plume 2) and 2b (plume 3) and Animations S1–S3). The same type of small instabilities will later develop also in the plume foot and travel upwards through the plume stem (Animation S1), as seen in numerical axisymmetric models [*Lin and van Keken, 2005*]. However, the fate of CDM in the plume depends on time since the instability cools as it ascends. As a result, the core of the plume head, which consists of initially hotter but chemically heavier material, can cool enough to become denser than the ambient fluid before reaching the surface of the tank: the heterogeneous material then stops (Figure 2a (plume 5)) or even sinks back (Figures 2a (plumes 6–9) and 2b (plumes 5–8) and Animations S2–S3). Separation occurs and a “secondary” thermal plume with a lower temperature anomaly (between 0.5 and 0.3 of the temperature anomaly of the composite plume) is generated from the top edge of the heavier collapsing blob (e.g., Figures 2a (plumes 6–7) and 2b (plumes 6–7) and Animations S2–S3). In this “failing-plume” phase, the thermo-chemical plumes fail to deliver most of the CDM to the surface and show various morphologies which are rarely axisymmetric (Figures 1–2). Only filaments of CDM are brought to the surface, dragged through viscous coupling by the secondary plume (Figures 2a (plumes 6–8), 2b (plumes 6–8), and 1d–1f). Meanwhile, CDM material in the thermo-chemical pile convects also on its own (Figures 1e–1g and Animation S2). When the plume bottom heat supply is disconnected, the hot pipe flow between the top and bottom boundary disappears with time, while the failing CDM blob still shows a significant temperature anomaly (Figure 2b (plume 8)).

### 3. Mantle Composite Plumes

[10] Figures 1 and 2 suggest that both the complexity of tomographic images under hotspots, and the time-dependence of hotspot characteristics could be explained by the diversity of morphology and stages observed in composite plumes.

[11] Despite the improving resolution of tomographic models, hot plume conduits deep in the mantle under hotspots should still be undetectable if they were only 50 to 100 km wide, as predicted by the classical purely thermal plume model [*Campbell and Griffiths, 1990*]. However, seismic imaging of the mantle beneath hotspots often reveals slow seismic velocity anomalies between 300 and 1000 km wide, and these anomalies are rarely continuous all the way from the core-mantle boundary (CMB) to the surface [e.g., *Montelli et al., 2006*]. For example, the mantle under Iceland show a contorted and patchy structure (Figure 3) which includes: a continuous strong slow seismic velocity anomaly in the upper mantle, seen in both regional [*Allen and Tromp, 2005*] and global tomography (Figure 3), a slow velocity anomaly in the mid-lower mantle which produces anomalies in the arrival directions of teleseismic P-waves [*Pritschard et al., 2000*], and an ultra-low velocity zone (ULVZ) at the CMB [*Helmlberger et al., 1998*]. The consistent appearance of these features in different tomographic models suggests that the slow anomaly beneath Iceland does not vary smoothly in amplitude over the depth of the mantle, and could even be disconnected (Figures 3c–3d).

<sup>1</sup>Auxiliary materials are available in the HTML. doi:10.1029/2008GL035079.

[12] If the present-day Iceland plume is variable in space, the geological record shows that its characteristics have also varied strongly through time. The first major phase of mafic magma emplacement  $\sim 60$  Ma ago, which affected a broad area from Baffin Island to the British Isles (Figure 3a), involved picritic magma with temperatures at least 240–300 K higher than normal mantle [Gill *et al.*, 1992]. By contrast, present-day Iceland results only from a moderate temperature anomaly, estimated from seismological data or geodynamic modeling between 50 and 125 K [Allen and Tromp, 2005; Vinnik *et al.*, 2005; Ribe *et al.*, 1995].

[13] Both the time-dependence of the volcanic activity, and the apparent absence of a continuous conduit deep in the mantle have been interpreted as evidence for the non-existence of mantle plumes and a shallow (300 km deep) Icelandic source [Foulger and Anderson, 2005]. Our experiments give another light: Iceland could be produced by a thermo-chemical plume arising from the bottom of the heterogeneous mantle. The large-scale volcanic event about 60 Ma would correspond to the “successful” generation of the composite plume (Figures 1b–1e). Given mantle characteristics (Table 1), it would typically have arisen out of a 100–300 km-thick TBL and its maximum lateral extent at birth could have reached 500–1000 km in diameter [Le Bars and Davaille, 2004b; Farnetani and Samuel, 2005; Lin and van Keken, 2005; Samuel and Bercovici, 2006]. Using our local buoyancy criterion ( $B_1 \leq 1$ ), the  $\Delta T_{\text{trap}} \sim 240\text{--}300$  K temperature anomaly reported at the Earth's surface [Gill *et al.*, 1992] implies a density anomaly of compositional origin  $\Delta\rho_{\text{Xeff}}/\rho \leq \alpha \cdot \Delta T_{\text{trap}} \sim 0.7\text{--}0.9\%$  (taking  $\alpha = 3 \times 10^{-5}$ ). The composite nature of the plume (out of a TBL constituted of both CDM and mantle above it) could explain the signature of several mantle components observed in the geochemical data [Chauvel and Hémond, 2000; Moreira *et al.*, 2001; Blichert-Toft *et al.*, 2005]. Then, both the apparent disconnection between strong slow seismic anomalies in the upper and lower mantle (Figure 3) and the decrease in temperature anomaly ( $\Delta T \sim 100$  K  $\sim \Delta T_{\text{trap}}/3$ ) of present-day Iceland suggest that the composite plume could presently be in its “failing” stage. In this case, the patch of slow seismic anomaly in the lower mantle, although still hotter than ambient mantle, could be sinking because it is chemically denser (similar to Figure 2). This would explain why the lower mantle contribution to the Icelandic swell dynamic topography is always found to be weak [Marquart *et al.*, 2007].

#### 4. Conclusions

[14] The thermal and compositional structure of a thermo-chemical plume changes with time and is quite irregular. In particular, it is not because a region is hot that it is buoyant and rising. This gives new insights on the recent results of mantle seismic tomography: a) “fat” (i.e., 500 km-thick) low-velocity conduits can be the signature of thermo-chemical plumes, and b) a low seismic velocity (i.e., hot) region can be the thermal signature of denser sinking material, contrarily to the classical view based on the purely thermal plume model.

[15] **Acknowledgments.** This work was supported by the international collaboration between IPGP and ERI, the DyETI program from INSU and the ANR grant BEGDY. We thank T. Yanagisawa for supporting our

TLCs experiments, and Steve Grand, Barbara Romanowicz, Jeroen Ritsema and Guust Nolet to have made available their tomographic models. This manuscript benefited from discussions with Manuel Moreira and Neil Ribe, and was further improved thanks to reviews from Norm Sleep and Michael Manga.

#### References

- Allen, R. T., and J. Tromp (2005), Resolution of regional seismic models: Squeezing the Iceland anomaly, *Geophys. J. Int.*, *161*, 373–386.
- Blichert-Toft, J., A. Agranier, M. Andres, R. Kingsley, J.-G. Schilling, and F. Albarède (2005), Geochemical segmentation of the Mid-Atlantic Ridge north of Iceland and ridge-hot spot interaction in the North Atlantic, *Geochem. Geophys. Geosyst.*, *6*, Q01E19, doi:10.1029/2004GC000788.
- Campbell, I. H., and R. W. Griffiths (1990), Implications of mantle plume structure for the evolution of flood basalts, *Earth Planet. Sci. Lett.*, *99*, 79–93.
- Chauvel, C., and C. Hémond (2000), Melting of a complete section of recycled oceanic crust: Trace element and Pb isotopic evidence from Iceland, *Geochem. Geophys. Geosyst.*, *1*, 1001, doi:10.1029/1999GC000002.
- Courtillot, V. E., A. Davaille, J. Besse, and J. Stock (2003), Three distinct types of hotspots in the Earth's mantle, *Earth Planet. Sci. Lett.*, *205*, 295–308.
- Davaille, A. (1999), Simultaneous generation of hotspots and superswells by convection in a heterogeneous planetary mantle, *Nature*, *402*, 756–760.
- Davaille, A., and J. Vatteville (2005), On the transient nature of mantle plumes, *Geophys. Res. Lett.*, *32*, L14309, doi:10.1029/2005GL023029.
- Davaille, A., E. Stutzmann, G. Silveira, J. Besse, and V. Courtillot (2005), Convective patterns under the Indo-Atlantic  $\llcorner$  box  $\lrcorner$ , *Earth Planet. Sci. Lett.*, *239*, 233–252.
- Farnetani, C. G., and H. Samuel (2005), Beyond the thermal plume paradigm, *Geophys. Res. Lett.*, *32*, L07311, doi:10.1029/2005GL022360.
- Foulger, G. R., and D. L. Anderson (2005), A cool model for the Iceland hotspot, *J. Volcanol. Geotherm. Res.*, *141*, 1–22.
- Gill, R. C. O., A. K. Pedersen, and J. G. Larsen (1992), Tertiary picrites in west Greenland: Melting at the periphery of a plume?, in *Magmatism and the Causes of Continental Break-Up*, edited by B. C. Storey *et al.*, *Geol. Soc. Spec. Publ.*, *68*, 335–348.
- Grand, S. P., R. D. van der Hilst, and S. Widiyantoro (1997), Global seismic tomography: A snapshot of convection in the Earth, *GSA Today*, *7*(4), 1–7.
- Griffiths, R. W., and I. H. Campbell (1990), Stirring and structure in mantle starting plumes, *Earth Planet. Sci. Lett.*, *99*, 66–78.
- Helmberger, D. V., L. Wen, and X. Ding (1998), Seismic evidence that the source of the Iceland hotspot lies at the core-mantle boundary, *Nature*, *396*, 251–255.
- Jellineck, A. M., and M. Manga (2002), The influence of a chemical boundary layer on the fixity, spacing and lifetime of mantle plumes, *Nature*, *418*, 760–763.
- Kumagai, I., A. Davaille, and K. Kurita (2007), On the fate of thermally buoyant mantle plumes at density interfaces, *Earth Planet. Sci. Lett.*, *254*, 180–193.
- Le Bars, M., and A. Davaille (2004a), Large interface deformation in two-layer thermal convection of miscible viscous fluids, *J. Fluid Mech.*, *499*, 75–110.
- Le Bars, M., and A. Davaille (2004b), Whole layer convection in a heterogeneous planetary mantle, *J. Geophys. Res.*, *109*, B03403, doi:10.1029/2003JB002617.
- Lin, S.-C., and P. E. van Keken (2005), Multiple volcanic episodes of flood basalts caused by thermochemical mantle plumes, *Nature*, *436*, 250–252.
- Marquart, G., H. Schmeling, and O. Čadež (2007), Dynamic models for mantle flow and seismic anisotropy in the North Atlantic region and comparison with observations, *Geochem. Geophys. Geosyst.*, *8*, Q02008, doi:10.1029/2006GC001359.
- Mégnin, C., and B. Romanowicz (2000), The 3D shear velocity structure of the mantle from the inversion of body, surface and higher mode waveforms, *Geophys. J. Int.*, *143*, 709–728.
- Montelli, R., G. Nolet, F. A. Dahlen, and G. Masters (2006), A catalogue of deep mantle plumes: New results from finite-frequency tomography, *Geochem. Geophys. Geosyst.*, *7*, Q11007, doi:10.1029/2006GC001248.
- Moreira, M., K. Breddam, J. Curtice, and M. D. Kurz (2001), Solar neon in the Icelandic mantle: New evidence for an undegassed lower mantle, *Earth Planet. Sci. Lett.*, *185*, 15–23.
- Morgan, W. J. (1971), Convection plumes in the lower mantle, *Nature*, *230*, 42–43.
- Morgan, W. J. (1978), Rodriguez, Darwin, Amsterdam, . . . , A second type of hotspot island, *J. Geophys. Res.*, *83*, 5355–5360.
- Namiki, A., and K. Kurita (1999), The influence of boundary heterogeneity in experimental models of mantle convection, *Geophys. Res. Lett.*, *26*(13), 1929–1932.

- Pritschar, M. J., G. R. Foulger, B. R. Julian, and J. Fyfe (2000), Constraints on a plume in the mid-mantle beneath the Iceland region from seismic array data, *Geophys. J. Int.*, *143*, 119–128.
- Ribe, N. M., Ú. R. Christensen, and J. Theissing (1995), The dynamics of plume-ridge interaction, 1: Ridge-centered plumes, *Earth Planet. Sci. Lett.*, *134*, 155–168.
- Richards, M. A., R. A. Duncan, and V. E. Courtillot (1989), Flood basalts and hot-spot tracks: Plume heads and tails, *Science*, *246*, 103–107.
- Ritsema, J., H. J. van Heijst, and J. H. Woodhouse (1999), Complex shear wave velocity structure imaged beneath Africa and Iceland, *Science*, *286*, 1925–1928.
- Samuel, H., and D. Bercovici (2006), Oscillating and stagnating plumes in the Earth's lower mantle, *Earth Planet. Sci. Lett.*, *248*, 90–105.
- Schubert, G., D. L. Turcotte and P. Olson (2001), *Mantle Convection in the Earth and Planets*, Cambridge Univ. Press, New York.
- Sleep, N. H. (1990), Hotspot and mantle plumes: Some phenomenology, *J. Geophys. Res.*, *95*, 6715–6736.
- Vinnik, L. P., G. R. Foulger, and Z. Du (2005), Seismic boundaries in the mantle beneath Iceland: A new constraint on temperature, *Geophys. J. Int.*, *160*, 533–538.
- Wilson, J. T. (1963), Evidence from islands on the spreading of ocean floor, *Nature*, *197*, 536–538.
- 
- A. Davaille, I. Kumagai, and E. Stutzmann, Institut de Physique du Globe de Paris, UMR7154, Université Paris Diderot, CNRS, 4 Place Jussieu, F-75252 Paris CEDEX 05, France. (kumagai@ipgp.jussieu.fr)
- K. Kurita, Earthquake Research Institute, University of Tokyo, 1-1-1, Yayoi, Bunkyo-ku, 113-0032 Tokyo, Japan.